applied optics

Measuring method of diffraction efficiency for plane grating based on Fourier spectral technology

Zhenyu Ma,[1,2] Xiangdong Qi,[1,*] Xiaotian Li,[1] Shanwen Zhang,[1] Bayanheshig,[1] Hongzhu Yu,[1] Haili Yu,[1] and Qingbin Jiao[1]

[1]Grating Technology Laboratory, Changchun Institute of Optics and Fine Mechanics and Physics, Chinese Academy of Sciences, Changchun, Jilin 130033, China
[2]University of Chinese Academy of Sciences, Beijing 100049, China
*Corresponding author: chinagrating@263.net

Received 2 September 2015; accepted 24 November 2015; posted 10 December 2015 (Doc. ID 249368); published 15 January 2016

A traditional double monochromatic measurement instrument of diffraction efficiency for a plane grating involves two major problems: one is the differences of output spectrum bandwidths during measurement of a standard reflection mirror and the tested grating; the other is overlapping of diffracted spectra, which influence testing accuracy of diffraction efficiency. In this paper, a new measuring method of diffraction efficiency based on Fourier spectral technology is presented. The mathematical model of diffraction efficiency is first deduced and then verified by ray tracing and Fourier optics simulation. The influences of the moving cube corner's tilt error, lateral shift error, and maximal moving distance error on the measurement accuracy are analyzed in detail. The analyses provide theoretical references for designing diffraction efficiency instruments. Compared with the traditional diffraction efficiency measurement instrument with double monochromator structure, our method not only improves the measurement accuracy of diffraction efficiency but also has the advantage of high luminous flux, high spectral resolution, multiwavelength measurement in mean time, and high wavenumber accuracy.

OCIS codes: (050.1950) Diffraction gratings; (120.4640) Optical instruments; (070.0070) Fourier optics and signal processing.

http://dx.doi.org/10.1364/AO.55.000522

1. INTRODUCTION

Diffraction efficiency [1], as one of the most important performance properties of plane diffraction grating [2–6], directly determines energy transmission characteristics of spectral instruments. Its measuring results can give guidance to grating fabrication technology and to accuracy analysis of a grating ruling engine [7–10]. Whatever for makers or users of grating, it is important to research and develop high-accuracy measurement devices of grating diffraction efficiency [11–13].

The measurement of diffraction efficiency for plane grating can be divided into absolute and relative measurement methods. The principle of the absolute measurement method is simple and easy to set up [14–16]. However, the results are only a rough estimation, and the detectable grating area is small and limited. Though Keller [17] established an absolute diffraction-efficiency detection method, which improved the detectable grating area and had the measuring accuracy about 3%, only some discrete wavelengths could be tested because no continuous laser lights were composed in his optical structure. Currently, most measurement instruments of relative diffraction efficiency for plane grating adopt a double monochromator structure: the first offers necessary monochromatic light for detection; the second measures diffraction efficiency at this wavelength [18,19]. Though the testing method is widely used, the first monochromator needs to be calibrated time and time again, and the single channel testing mode of double monochromator structure reduces measurement efficiency; furthermore, there exits different output spectrum bandwidths between the standard mirror and the tested grating and overlapping of diffracted spectra, which influence the testing accuracy of diffraction efficiency.

In this paper, a new measuring method of the relative diffraction efficiency for the plane grating based on Fourier spectral technology and its detailed mathematical model are both presented. We analyze the influence of the moving cube corner's tilt error, lateral shift error, and maximal moving distance error on the measurement accuracy in detail. Compared with the diffraction efficiency measurement instrument with double monochromator structure, this method can avoid the influence of bandwidth inconformity and overlaps of diffraction orders, thus improving the diffraction-efficiency measurement accuracy.

2. MATHEMATICAL MODEL

The diffraction-efficiency measurement structure of our proposed method is shown in Fig. 1. It mainly consists of a light source system, Fourier-spectrum measurement system based on Michelson interferometer structure, monochromator measurement system, and data-processing system. The complex lights offered by the light source system go through the entrance slit and enter into the Fourier spectrum measurement system, which turns the complex lights into interference light. Then, interference light goes through a monochromator measurement system and forms an interference pattern on the detector, as shown in Fig. 1.

The new measurement of grating diffraction efficiency can be realized in three steps. In the first step, a standard reflection mirror is placed on the rotation stage (see Fig. 1) at a certain angle so that relevant wavelengths of light can be received by the detector; then, the PZT translation stage is driven by a single period, so that the detector can gather the interferometer data at the same time. In the second step, put the tested grating on the rotation stage instead of the standard reflection mirror and rotated; then drive the PZT translation stage and gather the interferometer data just like in the first step. In the last step, the data are processed respectively, and the diffraction efficiency can be calculated at the end.

The mathematical model for calculating grating diffraction efficiency by this method is given as follows. According to the principle of Fourier spectral technology, when the tested grating and the standard mirror is respectively placed (see Fig. 1), the interference intensity received by the detector $I_g(x)$, $I_r(x)$ can be written as

$$\begin{cases} I_g(x) = \int B_g(\lambda)[1 + \cos\, 2\pi x/\lambda]\mathrm{d}x \\ I_r(x) = \int B_r(\lambda)[1 + \cos\, 2\pi x/\lambda]\mathrm{d}x \end{cases}, \tag{1}$$

where $B_g(\lambda)$ represents the input spectrum intensity at the wavelength λ when the tested grating is placed, $B_r(\lambda)$ stands for the input spectrum intensity at the wavelength λ when the standard mirror is placed, and x is the optical-path difference between two arms of the interferometer.

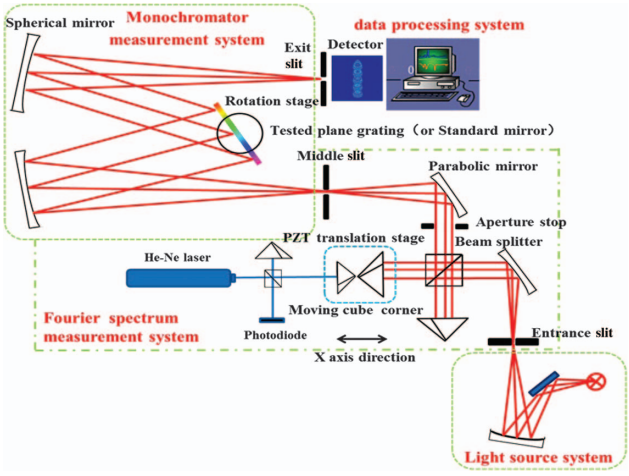

Fig. 1. Diagram of grating diffraction efficiency measurement system.

After the interference intensities $I_g(x)$, $I_r(x)$ are processed by the steps of DC component removal, apodization, phase correction, the processed interference intensities $I'_g(x)$, $I'_r(x)$ are obtained. According to the relationship among $I'_g(x)$, $I'_r(x)$, $B_g(\lambda)$, and $B_r(\lambda)$, Eq. (1) can be expressed as

$$\begin{cases} B_g(\lambda) = f_{\mathrm{FFT}}[I'_g(x)] \\ B_r(\lambda) = f_{\mathrm{FFT}}[I'_r(x)] \end{cases}, \tag{2}$$

where $f_{\mathrm{FFT}}[I'_g(x)]$ and $f_{\mathrm{FFT}}[I'_r(x)]$ are the Fourier transform of $I'_g(x)$ and $I'_r(x)$.

When the tested grating is placed on the rotated stage (see in Fig. 1), the input spectrum intensity $B_g(\lambda)$ is correlated with the spectrum intensity of the light source $B(\lambda)$, the reflectivity of the beam splitter $R(\lambda)$, the transmissivity of the beam splitter $T(\lambda)$, the total transmissivity of the instrument except the tested grating (or the standard mirror) and beam splitter $\tau(\lambda)$, the response functions of the detector $\chi(\lambda)$, the absolute diffraction efficiency of the tested grating $\eta(\lambda)$, the entrance-slit radius of the Fourier-spectrum measurement system r, the solid angles of output beam Ω_g, and the reducing spectrum bandwidth $\Delta\lambda_g$:

$$B_g(\lambda) = 2\pi r^2 \Omega_g R(\lambda) T(\lambda) \tau(\lambda) \eta(\lambda) \chi(\lambda) B(\lambda) \Delta\lambda_g. \tag{3}$$

When the tested grating is replaced by the standard mirror, the input spectrum intensity $B_r(\lambda)$ can be expressed as

$$B_r(\lambda) = 2\pi r^2 \Omega_r R(\lambda) T(\lambda) \tau(\lambda) \gamma(\lambda) \chi(\lambda) B(\lambda) \Delta\lambda_r, \tag{4}$$

where $\gamma(\lambda)$ is the reflectivity of the standard mirror, Ω_r is the solid angle of the output beam during measuring the standard mirror, and $\Delta\lambda_r$ is the bandwidth of the Fourier-reducing spectrum during measuring the standard mirror.

In the meantime, the relative diffraction efficiency $\eta_R(\lambda)$ can be expressed as

$$\eta_R(\lambda) = \frac{\eta(\lambda)}{\gamma(\lambda)}. \tag{5}$$

By combining Eqs. (2) to (5), we can deduce

$$\begin{cases} \eta_R(\lambda) = \frac{1}{k(\theta)} \cdot \frac{f_{\mathrm{FFT}}[I'_g(x)]}{f_{\mathrm{FFT}}[I'_r(x)]} \cdot \frac{\Delta\lambda_r}{\Delta\lambda_g} \\ k(\theta) = \frac{\Omega_g}{\Omega_r} \end{cases}, \tag{6}$$

where $k(\theta)$ is the diffraction cross-section factor.

To compute the relative diffraction efficiency $\eta_R(\lambda)$, the diffraction cross-section factor $k(\theta)$ should be decided. Figure 2 shows the schematic diagram of the cross-section area of the output beam, where S is the cross-section area of incident light, S_r is the cross-section area of the reflective light of the standard mirror, and S_g is the cross-section area of the diffractive light of the grating. Relationships among S, S_r, and S_g can be obtained:

$$\begin{cases} S_r = S \\ S_g = S \cdot \frac{\cos\beta}{\cos\alpha} \end{cases}, \tag{7}$$

where α and β are the incident angle and the diffractive angle of the grating.

According to Eqs. (6) and (7), the diffraction cross-section factor $k(\theta)$ can be acquired as

$$k(\theta) = \frac{\Omega_g}{\Omega_r} = \frac{S_g/f^2}{S_r/f^2} = \frac{\cos\beta}{\cos\alpha}, \tag{8}$$

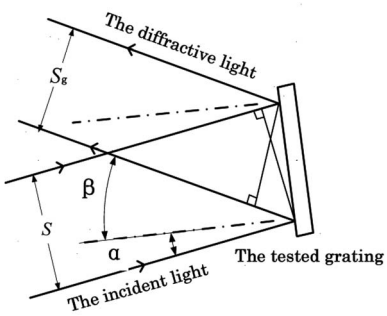

(a) Under the condition of the tested grating

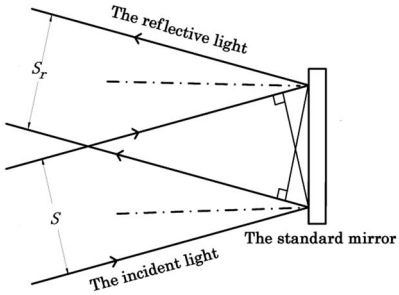

(b) Under the condition of the standard mirror

Fig. 2. Diagram of the cross-section area of the output beam.

where f is the focal length of the spherical mirror in front of the detector.

According to Eq. (6), just as in traditional diffraction efficiency measurement device, which needs to meet four measurement conditions to measure diffraction efficiency correctly, our proposed method needs to meet the following two measurement conditions: (a) the Fourier spectrum bandwidth should be less than the bandwidth of the monochromator measurement system at the exit slit. By enlarging the size of entrance slit and the travel of PZT, we can effectively increase the bandwidth of the monochromator measurement system at the exit slit and reduce the Fourier spectrum bandwidth. Thus, this testing condition can be easily met; (b) $\Delta\lambda_g = \Delta\lambda_r$, namely, the Fourier spectrum bandwidth during measuring the tested grating and the standard mirror must be the same. According to the principle of Fourier spectral technology, the Fourier spectrum bandwidth is only related to the maximum optical-path difference L. Thus, by keeping the maximum optical-path difference L the same, we can satisfy this condition.

When the above measurement conditions are met, Eqs. (6) and (8) can be combined and simplified as

$$\eta_R(\lambda) = \frac{\cos\alpha}{\cos\beta} \cdot \frac{f_{\mathrm{FFT}}[I'_g(x)]}{f_{\mathrm{FFT}}[I'_r(x)]}, \tag{9}$$

where $f_{\mathrm{FFT}}[I'_g(x)]$ and $f_{\mathrm{FFT}}[I'_r(x)]$ is the Fourier transform of $I'_g(x)$ and $I'_r(x)$.

Therefore, the relative diffraction efficiency can be finally obtained from Eq. (9) by acquiring the processed interference intensity $I'_g(x)$ and $I'_r(x)$ from the interference intensity $I_g(x)$ and $I_r(x)$.

3. SIMULATION OF THE MODEL

The ray tracing method is used to simulate the optical structure, the Fourier optics method is adopted to process the interferogram, and the correctness of our mathematical model is finally verified. After the standard mirror is placed on the rotated stage, and the PZT is driven to a certain position, an interferogram can be acquired, as shown in Fig. 3. Replacing the standard mirror by the tested grating, another interferogram can be acquired, as shown in Fig. 4. After driving the PZT to different positions along the positive (or negative) direction of the x axis (as shown in Fig. 1), lots of interferogram pairs can be collected, as shown in Figs. 3 and 4. Total powers of interferogram pairs under standard mirror and tested grating conditions are separately gathered.

After removing the direct-current component and using fast Fourier transformation, we can, respectively, obtain the spectrum curves under standard mirror and tested grating conditions (see Fig. 5). In Fig. 5, there are several peaks in the reducing spectrum in the whole detector (in our simulation model, the size of the detector is Φ18 mm, and there are seven peaks in the detector), so several values of the relative diffraction efficiency can be computed at the same time. Figure 6 shows only one peak of the reducing spectrum, which is part of Fig. 6. In order to compute the relative diffraction efficiency, the maximum values of the solid curve line and the dashed

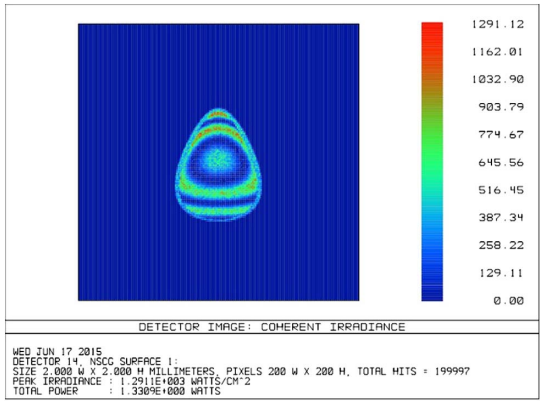

Fig. 3. Interferogram of new method with standard mirror.

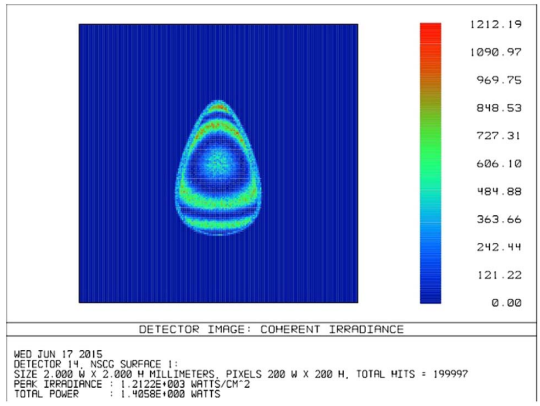

Fig. 4. Interferogram of new method with tested grating.

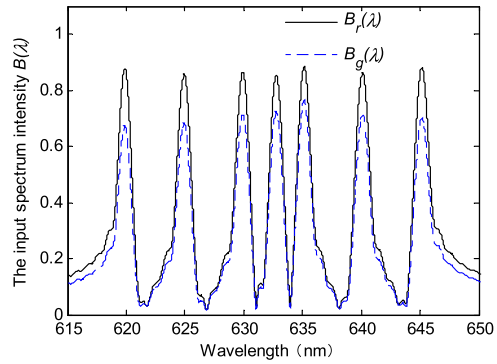

Fig. 5. Reducing spectrum diagram under the whole detector.

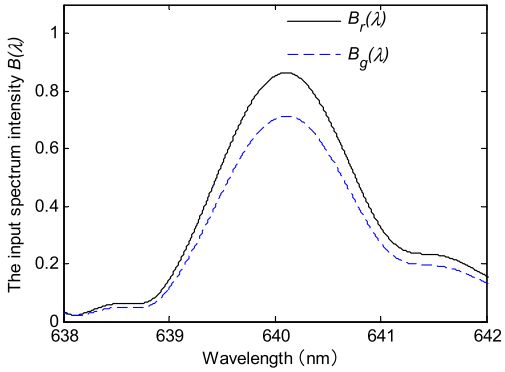

Fig. 6. Reducing spectrum diagram under part of the detector.

curve line in Fig. 6 are necessary to be respectively picked up. By computing the ratio of the above two maximum values, the value of relative grating diffraction efficiency $\eta_R(\lambda)$ is acquired. Because the reflectivity of the standard mirror $\gamma(\lambda)$ is known, the absolute diffraction efficiency $\eta(\lambda)$ can be acquired by Eq. (5). Table 1 gives the contrast between ideal absolute diffraction efficiency and simulated absolute diffraction efficiency under three different wavelengths. As shown in Table 1, simulated values of the diffraction efficiency agree well with the ideal values of the diffraction efficiency, meaning that our proposed method is correct and feasible.

Table 1. Contrast of Simulated and Ideal Diffraction Efficiencies

Wavelength (nm)	Relative Efficiency $\eta_R(\lambda)$ (%)	Simulated Absolute Efficiency $\eta(\lambda)$ (%)	Ideal Absolute Efficiency (%)
620	76.088	71.979	72
625	79.283	75.001	75
630	82.455	78.002	78
632.8	84.545	79.979	80
635	86.689	82.008	82
640	82.463	78.010	78
645	79.291	75.009	75

4. ERROR ANALYSIS

The simulation above is all based on the ideal situation, some factors such as the tilt error and lateral shift error of the moving cube corner, along with the error of the maximal moving distance, will have influence on the accuracy of the measurement result. Thus, it is necessary to analyze their effects on the measurement accuracy and limit their ranges of variation.

A. Tilt Error of the Moving Cube Corner

Assuming that D is the diameter of the parallel light in the Michelson interferometer structure, β_g is the tilt error of the moving cube corner when the tested grating is put into the light path, and β_r is the tilt error of the moving cube corner when the tested grating is instead by the standard mirror. If the moving cube corner exists in the tilt error, the modulation of interferometry intensity $M_r(\lambda)$ when the standard mirror is put into the light path is

$$M_r(\lambda) = \sin c(2\beta_r^2 D/\lambda). \tag{10}$$

For the same reason, the modulation of interferometry intensity $M_g(\lambda)$ when the tested grating is put into the light path is

$$M_g(\lambda) = \sin c(2\beta_g^2 D/\lambda). \tag{11}$$

Thus, Eq. (1) is changed to

$$\begin{cases} I_g(x) = B_g(\lambda)\{1 + M_g(\lambda)\cos[2\pi(x+\psi_g)/\lambda]\} \\ I_r(x) = B_r(\lambda)\{1 + M_r(\lambda)\cos[2\pi(x+\psi_r)/\lambda]\} \end{cases}, \tag{12}$$

where ψ_g is the additional optical-path difference compared with the ideal optical-path difference when the tested grating is placed, and ψ_r is the additional optical-path difference compared with the ideal optical-path difference when the standard mirror is placed.

By assuming that β_g and β_r remain the same during the whole moving process of the moving cube corner, the relative diffraction efficiency $\eta_R(\lambda)$ is

$$\eta_R(\lambda) = \frac{1}{k(\theta)} \cdot \frac{B_g(\lambda)}{B_r(\lambda)} \cdot \frac{M_g(\lambda)}{M_r(\lambda)}. \tag{13}$$

Combining Eqs. (2), (9), and (13), the relative error of relative diffraction efficiency ξ is

$$\xi = \left| \frac{M_g(\lambda)}{M_r(\lambda)} - 1 \right| = \left| \frac{\sin c(2\beta_g^2 D/\lambda)}{\sin c(2\beta_r^2 D/\lambda)} - 1 \right|. \tag{14}$$

By Eq. (14), the influence of the tilt errors (β_g and β_r) on the relative error of the relative diffraction efficiency ξ can be computed as shown in Fig. 7. In Fig. 7, we can see that the relative error of the relative diffraction efficiency ξ is less than 5×10^{-5}% when $|\beta_g|$ and $|\beta_r|$ are less than 30 arc seconds. Considering the tilt error of the PZT translation stage can be easily controlled within 30 arc seconds, the influence of the tilt errors of the moving cube corner on the relative error of the relative diffraction efficiency is negligible.

B. Lateral Shift Error of the Moving Cube Corners

According to the study of Murty [20], the lateral shift error of the moving cube corners causes the greatest decrease in modulation under the condition of the zero optical path difference, where the modulation $M_g(\lambda)$ and $M_r(\lambda)$ are given by

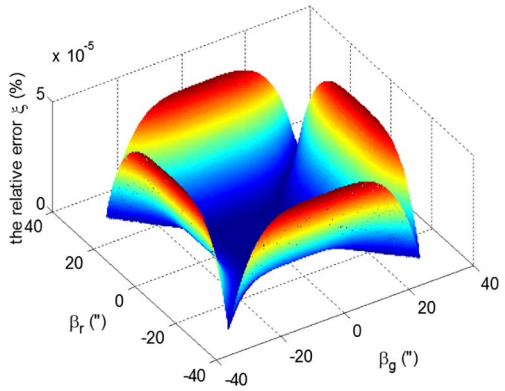

Fig. 7. Relative error ξ changed by the tilt error.

$$\begin{cases} M_g(\lambda) = \frac{2J_1(2\pi\varepsilon_g\omega_{\max}/\lambda)}{2\pi\varepsilon_g\omega_{\max}/\lambda} \\ M_r(\lambda) = \frac{2J_1(2\pi\varepsilon_r\omega_{\max}/\lambda)}{2\pi\varepsilon_r\omega_{\max}/\lambda} \end{cases}, \tag{15}$$

where ε_g and ε_r are the lateral shift errors of the moving cube corner when the tested grating and the standard mirror are separately put into the light path; $\omega_{\max}$ is the maximal field angle.

Combining Eqs. (12) and (15), the relative error of relative diffraction efficiency ξ is

$$\xi = \left|\frac{M_g(\lambda)}{M_r(\lambda)} - 1\right| = \left|\frac{\varepsilon_r J_1(2\pi\varepsilon_g w_{\max}/\lambda)}{\varepsilon_g J_1(2\pi\varepsilon_r w_{\max}/\lambda)} - 1\right|. \tag{16}$$

According to Eq. (16), when the lateral shift errors (ε_g and ε_r) are given a certain value and are unequal to each other, the relative error of relative diffraction efficiency ξ becomes smaller if the wavelength λ becomes longer (see Fig. 8). Thus, we only need to analyze the influence of the lateral shift errors on the relative diffraction efficiency ξ when the wavelength λ equals the minimal measurement wavelength. Figure 9 shows the influence of the lateral shift error of the moving cube corner (ε_g and ε_r) on the relative error of relative diffraction efficiency ξ when the wavelength λ equals 400 nm. Figure 10 is the contour line of Fig. 9. Judging from Fig. 10, we can find a rectangle region (similar to the dashed rectangle area shown in Fig. 10) in which the relative error ξ is always less than a certain value. For example, if we need the relative error ξ to be less than 0.4%, $|\varepsilon_g|$ and $|\varepsilon_r|$ should be both less than ~1.13 μm. Because the moving cube corner is fixed on the PZT translation stage, the above analysis will provide a theoretical reference for

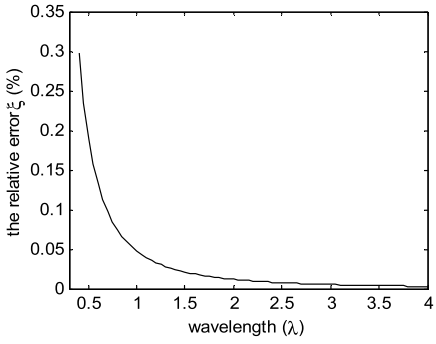

Fig. 8. Relative error ξ changed by the wavelength λ.

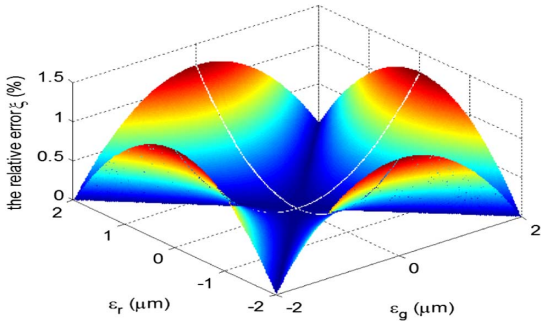

Fig. 9. Relative error ξ changed by the lateral shift error.

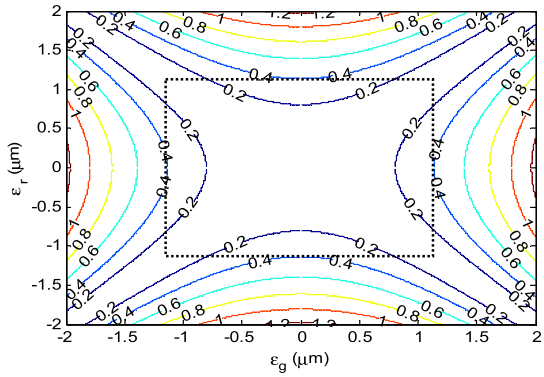

Fig. 10. Contour of relative error ξ changed by the lateral shift error.

confirming lateral shift error of the PZT translation stage of this method.

C. Error of the Maximal Moving Distance of the Moving Cube Corners

According to the principle of Fourier spectral technology, reducing spectrum bandwidth $\Delta\lambda$ can be similarly expressed as

$$\Delta\lambda \approx \lambda^2/L \tag{17}$$

L_g and L_r are assumed to be the maximal moving distance of the moving cube corners when the tested grating and the standard mirror are separately put into the light path. By combining Eqs. (6) and (17), the relative error of the relative diffraction efficiency ξ can be obtained as

$$\xi = \left|\frac{L_r}{L_g} - 1\right| = \left|\frac{\Delta L}{L_r - \Delta L}\right| \tag{18}$$

where ΔL is the difference between L_r and L_g.

By Eq. (18), we can compute the relative errors of the relative diffraction efficiency ξ changed by ΔL and L_r (see Fig. 11). The relative errors ξ can be reduced by enlarging L_r or by reducing ΔL. By using the PZT translation stage, we can easily control $|\Delta L|$ to be less than 1 μm. Thus, if the relative error of the relative diffraction efficiency ξ is needed to be smaller, the maximal moving distance of the moving cube corners (L_r or L_g) should be improved.

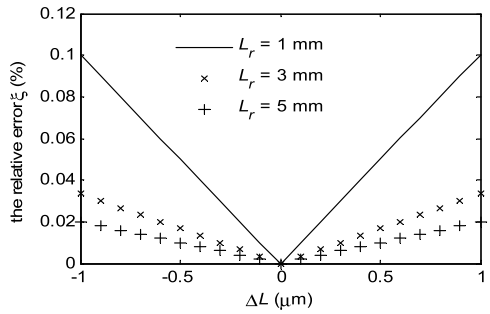

Fig. 11. Relative error ξ changed by ΔL.

5. DISCUSSION

Now, the main difference between our method and the traditional method with double monochromator structure is discussed.

A. Bandwidth

In the traditional method, the spectrum width $\Delta\lambda_g$ during measuring the tested grating can be expressed as

$$\Delta\lambda_g = f \cdot \frac{\partial\beta}{\partial\lambda} \cdot \Delta\lambda = \frac{f \cdot \Delta\lambda}{d \cos\beta}, \tag{19}$$

where $\Delta\lambda$ is the output bandwidth of the first monochromator, f is the focal distance of the focusing lens of the second monochromator, d is the grating constant, and β is the diffraction angle of the tested grating.

For the standard mirror, the spectrum bandwidth is the output bandwidth of first monochromator, namely, $\Delta\lambda_r = \Delta\lambda$. Thus, the traditional method cannot ensure the bandwidth conformity when the standard mirror and the tested grating are separately measured.

In the new method, we can approximately make $\Delta\lambda_g$ equal to $\Delta\lambda_r$ by minimalizing the error of the maximal moving distances during measuring the standard mirror and the tested grating. Thus, our new method can maximally ensure conformity of the bandwidths and improve the measurement accuracy of the diffraction efficiency.

B. High Luminous Flux and High Spectrum Resolution

In the traditional method, there is a mutual-restriction relationship between the output bandwidth $\Delta\lambda$ and the width of entrance slit of the first monochromator. To ensure the output spectral purity of the first monochromator, the entrance slit should be strictly limited, resulting in decreased input luminous flux. At present, the traditional method is used to measure the diffraction efficiency in our laboratory. Its first monochromator adopts a compact Czerny–Turner structure with output bandwidth of 2–4 nm and entrance slit width of 0.1 mm.

In the new method, the size of the entrance slit is not limited by the output bandwidth and only depends on the spectrum resolution and the size of the detector. The bandwidth can be less than 1 nm, and its entrance-slit diameter can reach to 1 mm in the spectral band from 0.4 to 2 μm. Obviously, compared with the traditional method, our proposed method has the advantages of high luminous flux and high spectrum resolution [21].

C. Multiwavelength Measurement at One Time

In the traditional method, only one wavelength can be measured at one time, while other wavelengths have to be measured by rotating the two gratings in the first and the second monochromators.

In the new method, the total measurement time can be remarkably reduced by the multiwavelength measurement at one time. Moreover, the band range in a single measurement can be broadened by selecting a large-area detector and reducing the focal length of spherical mirror in front of the detector. Supposing that the detector size is Φ18 mm, the simulation results show that we can simultaneously measure the diffraction efficiency in the range of more than $\pm$10 nm at the center wavelength in a single measurement.

D. Wavenumber Accuracy

In the traditional method, wavenumber accuracy depends on the rotation accuracy of the grating rotating mechanism in the first monochromator. For a sine mechanism, the relationship between wave number λ and the moving distance u is as follows:

$$\lambda = \frac{2d \cos(\varphi/2)u}{mL}, \tag{20}$$

where L is the length of the lever arm, m is the diffraction order, and φ is the angle between incident light and diffraction light.

According to Eq. (20), the relationship between wavenumber accuracy of the first monochromator and the minimum step distance of the rotating mechanism can be obtained. The wavenumber accuracy of the traditional method is generally at the level of 0.1 nm. Our method has a high wavenumber accuracy [22], however. By adopting equal-interval sampling and using a high-quality laser, the wavenumber accuracy of our method can reach to the level of 10^{-3} nm, which is 100 times more precise than the traditional method.

Additionally, the traditional method must be frequently calibrated, as its mechanical fray can cause the changes of wavelength. In our proposed method, we can realize real-time calibration by contrasting the reducing wavelength with the laser wavelength, thus finally improving automation level of the system.

E. Overlap of the Different Diffraction Orders

In the traditional method, the overlap of the diffracted spectra of the first monochromator would cause inaccuracy of the measured results. Our proposed method can completely separate the spectrum of the diffraction-order overlaps according to its wavelength by adopting Fourier spectrum technology, avoiding the influence of the diffraction-order overlaps on the measurement accuracy.

6. CONCLUSIONS

A new measurement method of diffraction efficiency for the plane grating is presented based on Fourier spectral technology. The mathematical model is elaborately deduced, and its principle is verified by ray tracing and Fourier optics simulation. The influence of the moving cube corner's tilt error, lateral shift error, and maximal moving distance error on the measurement accuracy is exhaustively analyzed. In comparison with the traditional method with double monochromator structure, our

proposed method can principally avoid the influence of bandwidth inconformity of output spectra between the standard mirror and the tested grating, along with the overlaps of diffraction orders. Entrance slit size can be enlarged 10 times over the traditional method under the condition of the high spectrum resolution, and its wavenumber accuracy can be 100 times more precise than in the traditional method. Our proposed method can simultaneously realize multiwavelength measurements to improve measurement efficiency (when the detector size is Φ18 mm, the diffraction efficiency in the range of ∼20 nm can be simultaneously measured in a single measurement). In short, our method not only improves the measurement accuracy of diffraction efficiency but also has the advantages of high luminous flux, high spectral resolution, multiwavelength measurement in mean time, and high wavenumber accuracy.

Funding. Chinese Finance Ministry (ZDYZ2008-1); Chinese Ministry of National Science and Technology (2014CB049500); Changchun Science and Technology Project (12ZX23); National Natural Science Foundation of China (NSFC) (61505204); Jilin Major Province Science & Technology Development Program Project (20140203011GX).

REFERENCES

1. R. F. Jarrell and G. W. Stroke, "Some new advances in grating ruling, replication, and testing," Appl. Opt. **3**, 1251–1261 (1964).
2. C. Vannahme, M. Dufva, and A. Kristensen, "High frame rate multiresonance imaging refractometry with distributed feedback dye laser sensor," Light: Sci. Appl. **4**, e269 (2015).
3. J. Qiao, F. Zhao, R. T. Chen, J. W. Horwitz, and W. W. Morey, "Athermalized low-loss echelle-grating-based multimode dense wavelength division demultiplexer," Appl. Opt. **41**, 6567–6573 (2002).
4. X. Du, C. Li, Z. Xu, and Q. Wang, "Accurate wavelength calibration method for flat-field grating spectrometers," Appl. Spectrosc. **65**, 1083–1086 (2011).
5. R. Kammel, R. Ackermann, J. Thomas, J. Gotte, S. Skupin, A. Tunnermann, and S. Nolte, "Enhancing precision in fs-laser material processing by simultaneous spatial and temporal focusing," Light: Sci. Appl. **3**, e169 (2014).
6. D. L. Voronov, M. Ahn, E. H. Anderson, R. Cambie, C.-H. Chang, E. M. Gullikson, and R. K. Heilmann, "High-efficiency 5000 lines/mm multilayer-coated blazed grating for extreme ultraviolet wavelengths," Opt. Lett. **35**, 2615–2617 (2010).
7. W. M. Burton and N. K. Reay, "Echelle efficiency measurements in the ultraviolet," Appl. Opt. **9**, 1227–1229 (1970).
8. E. Loewen, D. Maystre, E. Popov, and L. Tsonev, "Diffraction efficiency of echelles working in extremely high orders," Appl. Opt. **35**, 1700–1704 (1996).
9. X. Li, H. Yu, and X. Qi, "300 mm ruling engine producing gratings and echelles under interferometric control in China," Appl. Opt. **54**, 1819–1826 (2015).
10. C. Yang, X. Li, and H. Yu, "Practical method study on correcting yaw error of 500 mm grating blank carriage in real time," Appl. Opt. **54**, 4084–4088 (2015).
11. A. Bunkowski, O. Burmeister, P. Beyersdorf, K. Danzmann, and R. Schnabel, "Low-loss grating for coupling to a high-finesse cavity," Opt. Lett. **29**, 2342–2344 (2004).
12. I. G. Kuznetsov, E. Wilkinson, D. A. Content, R. A. Boucarut, and T. J. Madison, "Grating efficiencies comparison study: Calculations versus metrology for various types of high groove density gratings at VUV-UV wavelengths," Proc. SPIE **5178**, 267–277 (2004).
13. Y. Qu, S. Wang, Z. Zhang, and F. Li, "The second order diffraction efficiency measurements in the vacuum ultraviolet," Opt. Express **17**, 13187–13191 (2009).
14. M. C. Hutley, *Diffraction Grating* (Academic, 1982), p. 168.
15. J. F. Seely and L. I. Goray, "Efficiency of a grazing-incidence off-plane grating in the soft -x-ray region," Appl. Opt. **45**, 1680–1686 (2006).
16. P. Leclere, Y. Renotte, and Y. Lion, "Measure of the diffraction efficiency of a holographic grating created by two Gaussian beams," Appl. Opt. **31**, 4725–4733 (1992).
17. L. D. Keller, D. T. Jaffe, O. A. Ershov, T. Benedict, and U. U. Graf, "Fabrication and testing of chemically micromachined silicon echelle gratings," Appl. Opt. **39**, 1094–1101 (2000).
18. C. Palmer, *Diffraction Grating Handbook* (Newport Corporation, 2002), p. 174–175.
19. E. G. Loewen and E. Popov, *Diffraction Gratings and Applications* (Taylor & Francis, 1997), p. 413–417.
20. M. V. R. K. Murty, "Some more aspects of the Michelson interferometer with cube corners," J. Opt. Soc. Am. **50**, 7–10 (1960).
21. P. Jacquinot, "New developments in interference spectroscopy," Rep. Prog. Phys. **23**, 267–312 (1960).
22. J. Connes and V. Nozal, "Mathematical filtering in spectroscopy by the Fourier transformation," J. Phys. Radium **22**, 359–366 (1961).